

# Asymmetry of temporal cross-correlations in turbulent shear flows

By A. JACHENS,<sup>1</sup> J. SCHUMACHER,<sup>1</sup>  
 B. ECKHARDT,<sup>1</sup> K. KNOBLOCH<sup>2</sup>  
 AND H. H. FERNHOLZ<sup>2</sup>

<sup>1</sup>Fachbereich Physik, Philipps-Universität, D-35032 Marburg, Germany

<sup>2</sup>Hermann-Föttinger-Institut, Technische Universität, D-10623 Berlin, Germany

(Received 06 July 2005 and in revised form ??)

We investigate spatial and temporal cross-correlations between streamwise and normal velocity components in three shear flows: a low-dimensional model for vortex-streak interactions, direct numerical simulations for a nearly homogeneous shear flow and experimental data for a turbulent boundary layer. A driving of streamwise streaks by streamwise vortices gives rise to a temporal asymmetry in the short time correlation. Close to the wall or the bounding surface in the free-slip situations, this asymmetry is identified. Further away from the boundaries the asymmetry becomes weaker and changes character, indicating the prevalence of other processes. The systematic variation of the asymmetry measure may be used as a complementary indicator to separate different layers in turbulent shear flows. The location of the extrema at different streamwise displacements can be used to read off the mean advection speed; it differs from the mean streamwise velocity because of asymmetries in the normal extension of the structures.

---

## 1. Introduction

Coherent structures are very effective in transporting momentum across velocity gradients and thus contribute significantly to frictional drag in turbulent flows. Depending on the type of flow and the position of the layer being studied, different kinds of structures can be identified (Robinson, 1991; Panton 2001). In wall bounded shear flows, Robinson (1991) describes a dominance of streamwise vortices close to the walls and horseshoe-like structures in the outer region. For the intermediate region one might imagine a gradual transition in relative weight from one to the other. In transitional internal flows at low to intermediate Reynolds numbers streamwise vortices and streaks are also present (Eggels *et al.* 1994; Hof *et al.* 2004; Grossmann 2000), and a complete self-regenerating cycle for the dynamics, in which vortices drive streaks which then generate vortices through a shear instability, has been proposed (Waleffe 1997). The relation between internal and wall-bounded flow situations has been established through simulations in laterally confined geometries which show a similar dynamical behaviour (Hamilton *et al.* 1995). The presence of vortices and streaks in flows with homogeneous shear (Kida & Tanaka 1994; Schumacher & Eckhardt 2001) and calculations within rapid distortion theory (Nazarenko *et al.* 2000) highlight the significance of the background shear for their evolution and dynamics.

Streamwise streaks result from the mixing of fluid across the shear gradient as induced, for instance, by streamwise vortices. This is a linear process that suggests a causal relation between their appearance: the vortices have to be there first, and can then be followed

by the streaks. With the pointwise measurements in boundary layers in mind, we take velocity components as indicators for the structures: the streamwise turbulent velocity component  $u$  for the streaks and the wall-normal or shear component  $v$  for the vortices. The temporal correlation can then be verified for linear models of the vortex-streak interaction by direct calculation (Eckhardt & Pandit 2003). In particular, the model shows that the temporal cross-correlation function  $C_{vu}(\Delta t) = \langle u(t + \Delta t)v(t) \rangle_t$  will be asymmetric, and it will have its extremum at a finite time-delay  $\Delta t$ . The vortex as measured by  $v$  has a chance to influence the streak in  $u$  for  $\Delta t > 0$ , but not for  $\Delta t < 0$ . The question we address here is the extent to which this causal relation is reflected in an appropriate temporal correlation function in fully developed turbulent flows.

The correlations we are interested in can be obtained from two-point data, from measurements displaced in space or time or both. Apparently, the first such data were obtained by Blackwelder & Kovasznay (1972) in a turbulent boundary layer. Their correlations for  $y/\delta \approx 0.2$  † show a weak asymmetry of under  $\Delta t \rightarrow -\Delta t$ . Later, Blackwelder & Eckelmann (1978), studied cross-correlations between normal derivatives of the velocity components, and confirmed the asymmetry, as well as a shift in the maximum towards a positive time shift. Lagrangian studies of this cross-correlation along particle paths also show this asymmetry (Pope 2002).

Fully turbulent dynamics differs from the linear model with stochastic forcing by the presence of nonlinearities and a self-consistent generation of the turbulent fluctuations. In addition, the self-sustaining cycle proposed by Waleffe (1997) for the complete dynamics consists not only of the non-normal amplification but also of a linear instability that generates normal vortices which are then tilted into the streamwise direction by the main flow. The asymmetry is a property of the first part of the cycle, but not of the second. The correlation function of the full cycle will thus be a superposition of the contributions from the both parts, and the asymmetry will show up if the statistical weight of the second part is smaller than that of the first part.

With this in mind, we want to turn to the analysis of the cross-correlation functions of the turbulent velocity components for evidence of the dynamical processes underlying the self-sustaining mechanism for the formation of coherent structures. We will study in detail data from a low-dimensional model, from direct numerical simulations (DNS) of shear flows and from measurements with hot-wire probes in a boundary layer. The model allows for a detailed tracking of the dynamics of the various contributions to the spatial and temporal correlations. The DNS allows for an extension to two-point cross-correlations in space and time since they do not have to rely on Taylor's frozen flow hypothesis. Finally, the experimental data, although restricted to time asymmetry, allow for much higher Reynolds numbers and for a systematic study of the dependence of the correlation functions on the distance from the wall.

We take coordinates with  $x$  in streamwise,  $y$  in wall-normal and  $z$  in spanwise directions. The quantity we focus on is the correlation function between the normal velocity component  $v$  and the streamwise component  $u$ , displaced in the streamwise direction by  $\Delta x$  and in time by  $\Delta t$ ,

$$C_{vu}(\Delta t, \Delta x; y) = \frac{\langle v(x, y, z, t)u(x + \Delta x, y, z, t + \Delta t) \rangle_{x,z,t}}{\langle v(x, y, z, t)u(x, y, z, t) \rangle_{x,z,t}}. \quad (1.1)$$

The averages are over time and also over all points in an  $x$ - $z$ -plane at fixed height  $y$  (in

† Throughout this work, the boundary layer thickness  $\delta$  is defined as the distance between the wall and the height  $y$  where  $U = 0.99U_\infty$  with the free-stream velocity  $U_\infty$ .

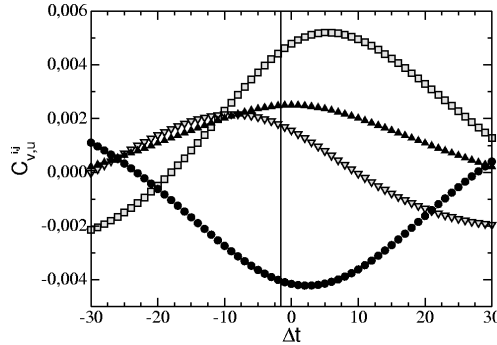


FIGURE 1. The time correlation function for the four modal pairs that contribute to the cross-correlation function in the nine-mode model:  $\blacksquare$  :  $C_{vu}^{8,6}$ ,  $\blacktriangledown$  :  $C_{vu}^{8,7}$ ,  $\blacktriangle$  :  $C_{vu}^{8,8}$ ,  $\bullet$  :  $C_{vu}^{3,2}$

the model and the DNS). Time correlations at one point are given by

$$\tilde{C}_{vu}(\Delta t; y) = C_{vu}(\Delta t, 0; y) = \frac{\langle v(x, y, z, t)u(x, y, z, t + \Delta t) \rangle_{x,z,t}}{\langle v(x, y, z, t)u(x, y, z, t) \rangle_{x,z,t}}. \quad (1.2)$$

In order to quantify the asymmetry effects we introduce the following measure for the temporal cross-correlations

$$Q_{vu}(\Delta t) = \frac{\tilde{C}_{vu}(\Delta t) - \tilde{C}_{vu}(-\Delta t)}{\tilde{C}_{vu}(\Delta t) + \tilde{C}_{vu}(-\Delta t)}, \quad (1.3)$$

(the dependence on height is suppressed in these expressions). For the extended correlations due to the non-normal amplification we expect  $|\tilde{C}_{vu}(\Delta t)| > |\tilde{C}_{vu}(-\Delta t)|$  such that  $Q_{vu} > 0$  for these cases.

The outline is as follows. In the next section, the low-dimensional model of a turbulent shear flow by Moehlis *et al.* (2004, 2005) is discussed. Section 3 describes the analysis of the DNS in a nearly homogeneous shear flow followed in section 4 by the discussion of boundary layer experiments of Knobloch & Fernholz (2004). Finally, a summary and an outlook are given.

## 2. Low-dimensional model of turbulent shear flow

The linear model of Eckhardt & Pandit (2003) can be extended to a nine-dimensional representation of shear flows, as discussed in more detail in Moehlis *et al.* (2004). The system is confined between two free-slip planes and driven by a volume force that sustains a laminar sinusoidal flow profile. The model captures the non-normal amplification process and completes it with modes for transversal shear and instabilities of the streamwise streaks. With  $L_y = d/2$ , the aspect ratio is  $L_x : L_y : L_z = 2\pi : 1 : \pi$ , and we simulate the flow at a Reynolds number  $Re = U_0 d / (2\nu) = 180$ , where the reference value for the velocity  $U_0$  is determined from the sustained laminar velocity profile at  $y = d/4$  with  $d$  being the distance between the free-slip planes.

With the Galerkin modes  $\mathbf{u}_i(\mathbf{x})$  and the amplitudes  $a_i(t)$  we can write the turbulent velocity field as

$$\mathbf{u}(\mathbf{x}, t) = \sum_{i=1}^N a_i(t) \mathbf{u}_i(\mathbf{x}). \quad (2.1)$$

The spatial part of the cross-correlations can be calculated analytically from the prescribed modes  $\mathbf{u}_i(\mathbf{x})$ . The temporal part follows from the numerical solution of a system

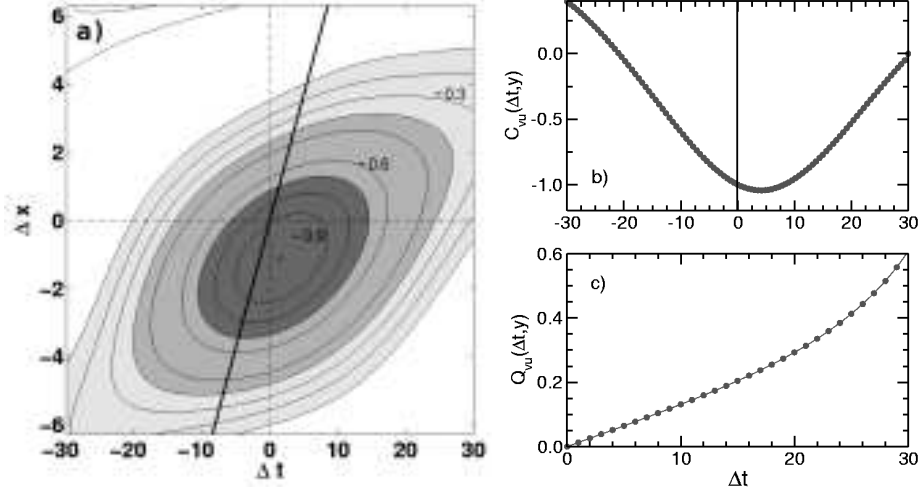


FIGURE 2. (a) Space-time cross-correlation  $C_{vu}(\Delta t, \Delta x; y)$  in the low-dimensional model taken at a height  $\tilde{y} = y/(d/2) = 0.52$ . The contour levels increase in steps of 0.1. The solid line represents the dimensionless mean velocity  $U(\tilde{y} = 0.52) = 0.74$ . (b) A cut through the contour plot in (a) at  $\Delta x = 0$  gives the temporal cross-correlation  $\tilde{C}_{vu}(\Delta t; y)$ . (c) Asymmetry measure  $Q_{vu}(\Delta t)$  corresponding to diagram (b). This measure is independent of  $y$  due to the spatial mode dependencies.

of ordinary differential equations for the  $a_i(t)$  that results with (2.1) from the Navier-Stokes equations. Equation (1.1) then becomes

$$C_{vu}(\Delta t, \Delta x; y) = \sum_{i,j=1}^N \langle a_i(t) a_j(t + \Delta t) \rangle_t \langle v_i(x, y, z) u_j(x + \Delta x, y, z) \rangle_{x,z}. \quad (2.2)$$

Of the 45 possible pairs of modes that could contribute to the correlation function only four terms, involving five modes, do. The modes that contribute are:  $\mathbf{u}_2$ , a streamwise streak with no streamwise variations;  $\mathbf{u}_3$ , a streamwise vortex;  $\mathbf{u}_6$  and  $\mathbf{u}_7$ , which describe two different wall-normal vortices; and  $\mathbf{u}_8$ , a mode that depends on all three coordinates. Thus  $C_{vu} = C_{vu}^{3,2} + C_{vu}^{8,6} + C_{vu}^{8,7} + C_{vu}^{8,8}$  where the superscripts indicate the particular mode couplings. Of these correlators,  $C_{vu}^{3,2}$  is exactly the one that probes the relation between streamwise vortices and streaks and therefore should have a significant variation with respect to  $\Delta t$ . This is indeed the case, as Fig. 1 shows.

When all contributions are collected, the space-time contours for  $C_{vu}(\Delta t, \Delta x; y)$  at  $y/(d/2) = 0.52$  are obtained (Fig. 2). The time correlations at a fixed position correspond to a cut along  $\Delta x = 0$  (cf. Fig. 1b) and the space correlations for fixed time from a cut at  $\Delta t = 0$ . The time correlation function is negative, as is to be expected for a flow where the streamwise velocity increases in the positive  $y$ -direction. It is asymmetric and the asymmetry gives a positive  $Q$  in the center of the layer. Because of the small number of modes in the system a more detailed dynamical system study is possible. An analysis of the periodic orbits in Moehlis *et al.* (2005) shows that some of them clearly follow the vortex-streak-instability sequence, but several do not. Nevertheless, the correlation functions in Fig. 2 show that the temporal asymmetry expected from the non-normal amplification process persists even after taking time averages.

Besides this similarity, there are differences to the linear model. The contour levels (Fig. 1a) show a global minimum that is shifted from the origin toward  $(\Delta t, \Delta x) \approx (1, -1)$  for this particular height. The shift in time stems from the streak-vortex coupling

---

	$N_x \times N_y \times N_z$	$L_x : L_y : L_z$	$U$	$S$	$\epsilon$	$u_{rms}$	$S^*$	$R_\lambda$
DNS-1	$128 \times 65 \times 128$	$2\pi : 1 : 2\pi$	1	2	0.04	0.37	6.1	79
DNS-2	$256 \times 129 \times 256$	$2\pi : \pi : 2\pi$	$3/\pi$	$6/\pi$	0.44	1.08	5.0	166

---

TABLE 1. Parameters of the two DNS that were taken for the analysis.  $U$  is the mean streamwise velocity at the free-slip boundary. The mean energy dissipation rate is given by  $\epsilon = 15\nu\langle(\partial u/\partial x)^2\rangle$ , as in the experimental determinations.  $S = dU/dy$  is the constant shear rate. The root mean square velocity is given by  $u_{rms} = \langle u^2 \rangle^{1/2}$ , the dimensionless shear parameter is  $S^* = Su_{rms}^2/\epsilon$  and the Taylor microscale Reynolds number  $R_\lambda = \sqrt{15/(\nu\epsilon)}u_{rms}^2$ . The spectral resolution criterion  $k_{max}\eta > 1$  is satisfied with  $k_{max} = \sqrt{2}N_x/3$ .

---

contributions  $C_{vu}^{3,2}$  and  $C_{vu}^{8,6}$ , and is compatible with the stochastic model (Eckhardt & Pandit 2003). The one in position can be traced back to the coupling of mode 8 with itself,  $\langle v_8(x, y, z)u_8(x + \Delta x, y, z) \rangle_{x,z} = \pi/(5 + \pi^2) \sin(\Delta x/2) \sin(\pi y)$  for  $-1 < y < 1$ . The space-time contours are elongated along an axis whose slope has dimensions of velocity. This velocity is not the mean velocity at the height of the measurement. As we will show below, this is due to an asymmetry in the width of the structures in the normal direction.

### 3. Nearly homogeneous shear flow

The direct numerical simulations of a turbulent shear flow also refer to a flow bounded by two parallel free-slip plates, driven by a volume force that sustains a linear shear flow in the mean,  $U(y) = Sy$ , except for a small boundary layer near the plates. Details of the numerical simulations are given in Schumacher & Eckhardt (2000) and Schumacher (2004). Relevant parameters for the simulation are listed in table 1.

Space-time contours for the cross-correlations in run DNS-1 are shown in Fig. 3a. Several features are similar to the ones in the low-dimensional model: it has the same asymmetry with respect to time and the iso-countours are oval and not aligned with the coordinate axis. Thus, even though more spatial degrees of freedom are present, the Reynolds number is higher, and the turbulence is fully developed, the non-normal amplification is reflected in the Eulerian cross-correlation function.

However, there are noticeable additional features. The asymmetry measure shows a pronounced height dependence, being strongest close to the bounding surfaces and getting weaker towards the center. In addition, it shows a time interval where its value is negative,  $Q_{uv} < 0$  (see Fig. 3c). This interval is almost negligible close to the walls and becomes longer as the reference position moves towards the center. We see this phenomenon linked to the difference in the number of modes that can contribute, and hence to the possibility of additional dynamical processes. Assuming that the smallest scale is set by dissipation and does not vary much across the flow, the largest scale for the possible structures is set by the distance to the free-slip boundary. By this reasoning there are fewer active modes close to the wall than in the center, thus limiting the nonlinear interactions and highlighting their correlations.

A spatial plot of the streamwise turbulent velocity component  $u$  and the shear component  $v$  in the  $x$ - $z$  plane for one point in time and at a fixed height  $y$  in the layer (see Fig. 4) reveals that the contributions to the cross-correlation function come from fragmented regions, of an extension compatible with the dimensions of coherent structures. Negative contours of  $v$  indicate streamwise vortices which generate the streamwise streaks (shown as gray-filled contours of  $u$ ). The maxima of  $u$  and  $v$  contours are displaced slightly, in

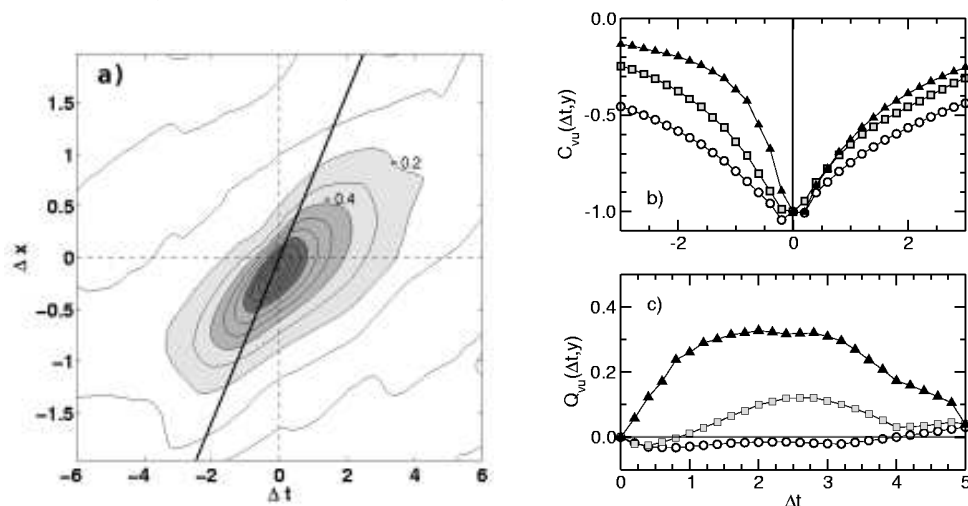


FIGURE 3. Space-time cross-correlation  $C_{vu}(\Delta t, \Delta x; y)$  of a nearly homogeneous shear flow. Data are taken from DNS-1 (see table 1) at a height  $y/L_y = 0.11$ . The Reynolds number  $Re = UL_y/\nu = 1800$  where  $U$  is the mean turbulent velocity at the boundary. (a) Space-time plot of the cross-correlations. The contours increase in steps of 0.1 and the unit value is at the origin. The solid line represents the dimensionless mean turbulent velocity  $U(y/L_y = 0.11) = 0.77$ . (b) Temporal cross-correlation along  $\Delta x = 0$  for different heights:  $\blacktriangle$  :  $y/L_y = 0.13$ ,  $\blacksquare$  :  $y/L_y = 0.25$ ,  $\circ$  :  $y/L_y = 0.50$ . (c) Asymmetry coefficient for  $\tilde{C}_{vu}(\Delta t; y)$  at the same heights as (b).

accordance with the off-set in the maximum of the spatial cross-correlation in Figs. 2a and 3a.

The off-set can be explained by the observation that a streamwise vortex pair centered at height  $y$  will be advected with the corresponding mean streamwise velocity at that height,  $U(y)$ . The pair will mix slower moving fluid into a region that moves on average faster, and hence will temporarily reduce the local advection velocity  $U_c$  to values below the mean velocity  $U(y)$ . But since  $U_c$  will advect the streamwise streak that is about to be lifted up, it will remain behind the vortex pair, resulting in the spatial shift of the most intense cross-correlation.

The correlation functions shown in Fig. 2 and 3 and many others for different aspect ratios and Reynolds number show an inclination of the isocountours in the spatio-temporal correlations  $C_{vu}(\Delta t, \Delta x; y)$ . Since the two axes being compared have dimensions of time and length, the inclination has the dimension of a velocity: but as the comparison with the straight lines in both figures shows, the velocity with which these structures are advected is systematically lower than the mean velocity at that height,  $U(y)$ . We can trace this effect back to an asymmetry of the spatial autocorrelation function of the streamwise turbulent velocity in the normal direction, as measured by

$$C_{uu}(\Delta y; y_0) = \langle u(x, y_0, z, t)u(x, y_0 + \Delta y, z, t) \rangle_{x,z,t}. \quad (3.1)$$

The left and middle diagram of Fig. 5 show that this function is asymmetric with respect to the wall-normal direction, obviously influenced by the presence of the free-slip walls at  $y = 0$  and  $y = L$ . If we estimate the mean advection speed of the coherent structures from an average of the streamwise speed over a domain determined by the full width at

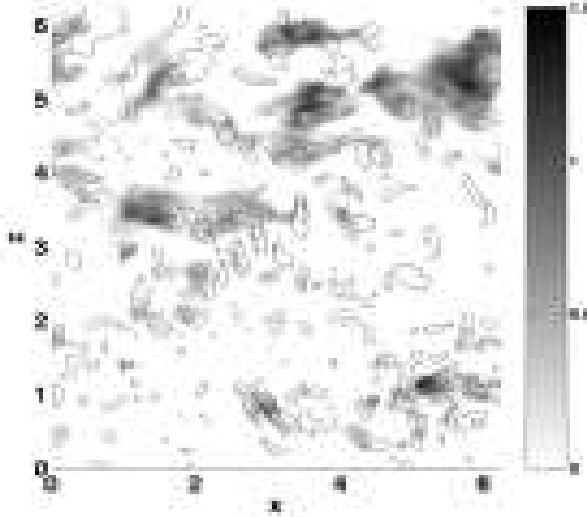


FIGURE 4. Snapshot of the two turbulent velocity fields entering the cross-correlation function. A slice cut from a sample of DNS-2 (see table 1) is taken. The turbulent streamwise velocity  $u$  is indicated by shading for values of  $u$  between 0 and 1.5, only. The contour lines show three isolevels of the wall-normal component  $v$  at values of  $-0.8$ ,  $-0.5$  and  $-0.2$ . The maxima are shifted relative to each other by a small streamwise distance that corresponds with the shift of the maximum of the space-time cross-correlation by  $\Delta x$  as visible in Fig. 3a.

half maximum of  $C_{uu}(\Delta x, \Delta y; y_0)$ , we find

$$U_c = \frac{1}{\ell_2 - \ell_1} \int_{\ell_1}^{\ell_2} U(y) dy. \quad (3.2)$$

Here,  $\ell_2$  and  $\ell_1$  are the widths at half maximum of the asymmetric  $C_{uu}(\Delta x = 0, \Delta y; y_0)$  (see also the mid diagram of Fig. 5). The result of such an averaging procedure can be seen in the right diagram of Fig. 5. The convection velocity as defined by (3.2) becomes smaller as the mean velocity and coincides with the inclination of the space-time contours of the velocity cross-correlations of Fig. 3. The coherent structures thus move with the streamwise speed as determined by an average over their size.

#### 4. Turbulent boundary layer

The third class of flows for which we determine cross-correlation functions are high-Reynolds number boundary layer flows. The experiments were done at a wind tunnel of the Hermann-Föttinger Institute (HFI) in Berlin and the German-Dutch Windtunnel (DNW). Triple hot-wire probes allowed measurements of all three velocity components. With sampling rates of 20 kHz at HFI and 125 kHz at DNW, data sets containing about a million data points at the HFI and 5 million at the DNW could be obtained. The boundary layer thickness (see the footnote on p. 3) was found to be  $\delta = 63\text{mm}$  at HFI and  $\delta = 240\text{mm}$  at DNW. Some parameters are summarized in table 2; further experimental details may be found in Knobloch & Fernholz (2004).

Because of the measurements at a single location, only the short time behaviour of the cross-correlation functions can be determined. The results for different distances from the wall and different Reynolds numbers are shown in Fig. 6. Already for the data set closest to the wall there is a time interval with negative values in the asymmetry measure,

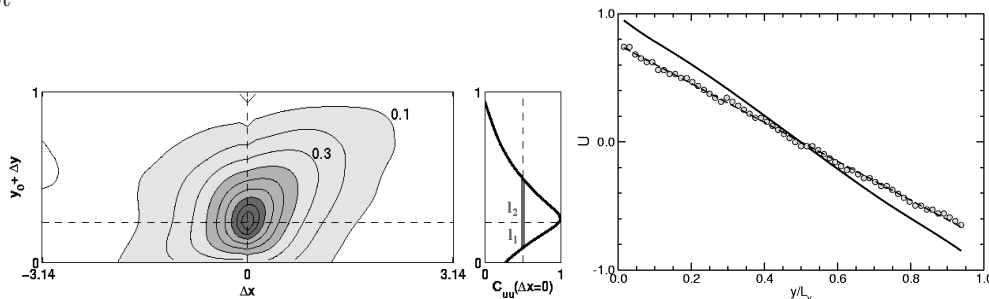


FIGURE 5. Left: Contour plot of spatial autocorrelation function  $C_{uu}(\Delta x, \Delta y; y_0)$  as given by (3.1) in streamwise and wall-normal directions taken at  $y_0 = 1/4$  from DNS-1. The inclination of this structure is about 9 degrees. Mid: A cut through the contour at  $\Delta x = 0$  is shown. It is also indicated how the two widths at half of the maximum,  $\ell_1$  and  $\ell_2$ , of the resulting autocorrelation function are defined. Right: Comparison of the mean ( $U$ ) and the convection ( $U_c$ ) velocities for data from DNS-1. Black solid line is for mean velocity as a function of the wall-normal distance  $y$ . The symbols stand for the corresponding convection velocity as given by (3.2).

and this interval increases as one moves further out. Comparison with the homogeneous shear flow DNS suggests that this point is already in the transition region away from the vortex dominated near wall layer. For the points furthest from the wall no reversal to positive values is detected.

The data from HFI and DNW are collected at about the same relative positions when heights are measured in units of the boundary layer thickness,  $y/\delta$ . The asymmetries at these heights show remarkably similar behaviour, especially for the value  $\tilde{y} = y/\delta = 0.11$ , which is present in both data sets, and for the two similar values  $\tilde{y} = y/\delta = 0.31$  (HFI) and  $0.34$  (DNW). In wall units, the  $\tilde{y} = 0.11$  corresponds to a height of  $y^+ \sim 174$  for the HFI data and  $y^+ \sim 3950$  for the DNW data. In agreement with the findings of De Graaff & Eaton (2000) and Del Alamo et al. (2003) for turbulent intensities, the cross-correlations collapse in external scaling, i.e. relative to boundary layer thickness and the external velocity. A possible explanation for this behaviour could be that the intermittent bursting activity in the boundary layer lifts fragments of the coherent structures higher into the intermediate layer, where their further breakup is determined by the boundary layer thickness  $\delta$  (see e.g. Blackwelder & Kovaszany 1972). Analysis of additional data shows that the asymmetry in the time correlations shows up for positions up to  $y = 0.05\delta$ .

Information about the instantaneous in-plane correlations similar to Fig. 5a can be obtained from PIV measurements at fixed heights. The data in Fig. 7 show that the inclination in  $C_{uu}(\Delta x, \Delta y; y_0)$  is preserved and has about the same value.

## 5. Summary

A comparison between the three sets of data shows that the vortex-streak interaction is reflected most strongly in the cross-correlation function closest to the wall or to bounding surfaces. Further away the signal gets weaker, as expected by the change in structures (Robinson 1991). The similarity of the asymmetry measure further out suggests the prevalence of a similar dynamics. Interestingly, the asymmetry measures are similar when the height is measured in units of boundary layer thickness, rather than viscous length scales. It will be interesting to see how horseshoe vortices and their dynamics are reflected



---

	$y/\delta$	$y^+$	$U_\infty$ [m/s]	$S$ [1/s]	$\epsilon$ [m <sup>2</sup> /s <sup>3</sup> ]	$u_{rms}$ [m/s]	$S^*$	$R_\lambda$
HFI	0.02	34	10	1576	39.6	0.97	37.8	151
	0.11	174	10	143	10.6	0.75	7.5	172
	0.31	519	10	72	4.7	0.64	6.4	192
DNW	0.02	709	80	1447	1146.4	6.31	50.3	1156
	0.11	3953	80	242	320.6	5.35	21.6	1574
	0.34	12507	80	109	123.6	4.27	16.1	1614

---

TABLE 2. List of boundary layer measurements. We have picked three distances from the wall for every free-stream velocity  $U_\infty$ .  $y^+ = yu_\tau/\nu$  with  $u_\tau = (\tau_{wall}/\rho)^{1/2}$ . The other quantities are defined as in the caption of Table 1.

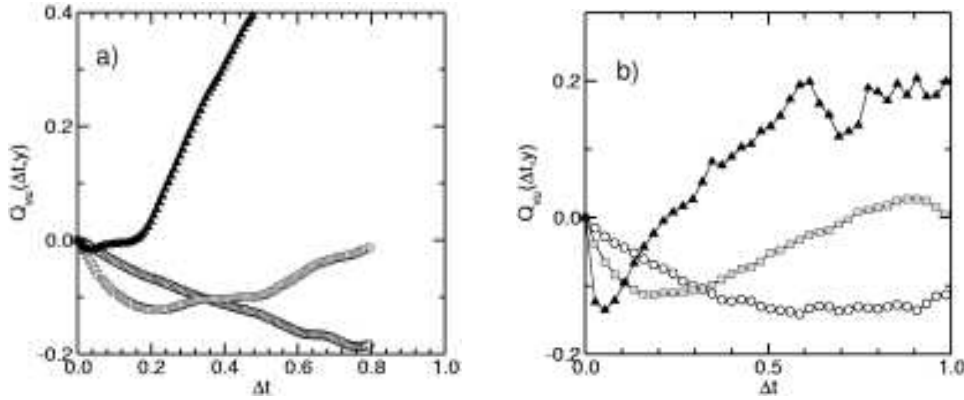


FIGURE 6. Asymmetry coefficient  $Q_{vu}(\Delta t)$  for two sets of turbulent boundary layer data. Time is given in units of  $\delta/U_\infty$  for both figures. (a): HFI measurement at  $Re_\delta = 41600$  for three different heights  $\tilde{y} = y/\delta$  above the wall,  $\blacktriangle$  :  $\tilde{y} = 0.02$ ,  $\blacksquare$  :  $\tilde{y} = 0.11$  and  $\circ$  :  $\tilde{y} = 0.31$ . (b): DNW measurement at Reynolds number  $Re_\delta = 1237900$ . Here  $\blacktriangle$  :  $\tilde{y} = 0.02$ ,  $\blacksquare$  :  $\tilde{y} = 0.11$  and  $\circ$  :  $\tilde{y} = 0.34$  (see also table 2 for more details).

in correlation functions, and whether they can explain the cross-correlation functions or whether other dynamical processes have to be identified.

The work was supported by the Deutsche Forschungsgemeinschaft (DFG) within the Interdisciplinary Turbulence Initiative, and by the DAAD within the PROCOPE program. We thank the John von Neumann Institute for Computing at the Forschungszentrum Jülich for continued computer access and support.

#### REFERENCES

- DEL ÁLAMO, J. C., JIMÉNEZ, J., ZANDONADE, P. & MOSER, R.D. Scaling of the energy spectra of turbulent channels. *J. Fluid Mech.* **500**, 135-144.
- BLACKWELDER, R. F. & KOVASZNY, L. S. G. 1972 Time scales and correlations in a turbulent boundary layer. *Phys. Fluids* **15**, 1545-1554.
- BLACKWELDER, R. F. & ECKELMANN, H. 1978 The spanwise structures of the bursting phenomenon. *Structure and mechanisms in turbulence I: Proceedings of the Symposium on Turbulence held at the Technische Universität Berlin 1977*, ed. by H. Fiedler, Springer, 190-204.

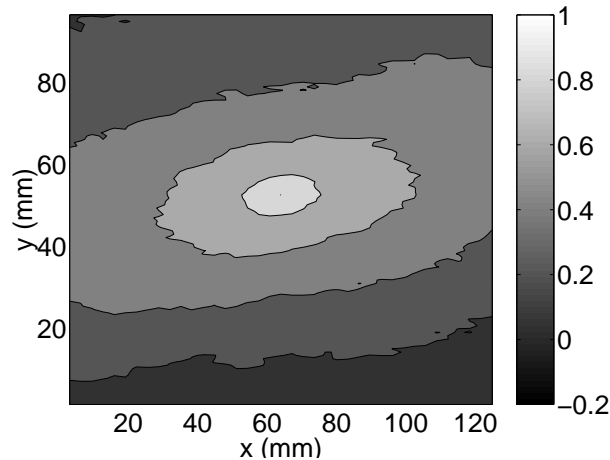


FIGURE 7. Contour plot of spatial autocorrelation function  $C_{uu}(\Delta x, \Delta y; y_0)$  as given by (3.1) in streamwise and wall-normal directions taken at  $y_0/\delta = 0.21$  from PIV measurements at the DNW. The inclination of this structure is about 11 degrees and similar to that in the boundary layer.

- DE GRAAFF, D.B. & EATON, J.H. 2000 Reynolds-number scaling of the flat-plate turbulent boundary layer. *J. Fluid Mech.* **422**, 319-346.
- ECKHARDT, B. & PANDIT, R. 2003 Noise correlations in shear flows. *Eur. Phys. J. B* **33**, 373-378.
- EGGELS, J. G. M., UNGER, F., WEISS, M. H., WESTERWEEL, J., ADRIAN, R. J., FRIEDRICH, R. & NIEUWSTADT, F. T. M. 1994 Fully developed turbulent pipe flow: a comparison between direct numerical simulation and experiment. *J. Fluid Mech.* **268**, 175-209.
- GROSSMANN, S. 2000 The onset of shear flow turbulence. *Rev. Mod. Phys.* **72**, 603-618.
- HAMILTON, J. M., KIM, J. & WALEFFE, F. 1995 Regeneration mechanisms of near-wall turbulence structures. *J. Fluid. Mech.* **287**, 317-348.
- HOF, B., VAN DOORNE, C. W. H., WESTERWEEL, J., NIEUWSTADT, F. T. M., FAISST, H., ECKHARDT, B., WEDIN, H., KERSWELL, R. R. & WALEFFE, F. 2004 Experimental observation of nonlinear travelling waves in a turbulent pipe flow. *Science* **305**, 1594-1598.
- KIDA, S. & TANAKA, M. 1994 Dynamics of structures in a homogeneous shear flow. *J. Fluid. Mech.* **274**, 43-68.
- KNOBLOCH, K. & FERNHOLZ, H. H. 2004 Statistics, correlations and scaling in a turbulent boundary layer at  $Re_{\delta_2} \leq 1.15 \times 10^6$ . *IUTAM Symposium on Reynolds Number Scaling in Turbulence* Princeton 2002, Kluwer Academic Publishers, 11-16.
- MOEHLIS, J., FAISST, H. & ECKHARDT, B. 2004 A low-dimensional model for turbulent shear flows. *New J. Phys.* **6**, 56 (17 pages).
- MOEHLIS, J., FAISST, H. & ECKHARDT, B. 2005 Periodic orbits and chaotic sets in a low-dimensional model for shear flows. *SIAM J. Appl. Dyn. Systems* **4**, 352-376.
- NAZARENKO, S., KEVLAHAN, N. K. R. & DUBRULLE B. 2000 Nonlinear rapid distortion theory of near-wall turbulence. *Physica D* **139**, 158-176.
- PANTON, R. L. 2001, Overview of the self-sustaining mechanisms of wall turbulence. *Prog. Aerospace Sci.* **37**, 341-383.
- POPE, S. B. 2002, Stochastic Lagrangian models of velocity in homogeneous turbulent shear flow. *Phys. Fluids* **14**, 1696-1702.
- ROBINSON, S. K. 1991 Coherent motions in the turbulent boundary layer, *Ann. Rev. Fluid Mech.* **23** 601-639.
- SCHUMACHER, J. & ECKHARDT, B. 2000 On statistically stationary homogeneous shear turbulence. *Europhys. Lett.* **52**, 627-632.
- SCHUMACHER, J. & ECKHARDT, B. 2001 Evolution of turbulent spots in a parallel shear flow. *Phys. Rev. E* **63**, 046307 (9 pages).

SCHUMACHER, J. 2004 Relation between shear parameter and Reynolds number in statistically stationary turbulent shear flows. *Phys. Fluids* **16**, 3094-3102.

WALEFFE, F. 1997 On a self-sustaining process in shear flows. *Phys. Fluids* **9**, 883-900.